Pattern Formation in Vertically Vibrated Nails

by

T. Lynn MacDonald

A project report submitted in conformity with the requirements
for the degree of Master of Science
Graduate Department of Physics
University of Toronto

Abstract

Pattern Formation in Vertically Vibrated Nails

T. Lynn MacDonald

Master of Science

Graduate Department of Physics

University of Toronto

2010

We report the experimental observation of pattern formation in vertically vibrated nails. Phase diagrams are drawn as a function of packing fraction and signal generator driving voltage for two different aspect ratios. Aspect ratio is shown to affect the states of order observed in the system. We investigate the behaviour of patterns in nails with head-tail orientation in full layers at 100% packing fraction as the driving voltage is increased in increments over time. Calculations of nematic and antiferromagnetic order parameters from data derived using manual and semi-automated nail detection from images taken as a function of driving voltage and time are performed.

Dedication

To Kyle, Michelle, and Jonathan, for acceptance of change. To Jack, for everything.

Acknowledgements

There are three groups of people I would like to thank for their part in making my return to academia and the completion of this project possible.

First, I need to thank those who enabled me to return to univeristy after a fifteen-year hiatus: Theodore Shepherd for encouraging me to apply when I first contacted him about the possibility in January 2009, and to Douglas Dahn and Edward Lank for being references to my ability after all this time.

Next, I thank people in my personal life: my extended family for being so understanding and supportive of such a major change in their lives, and to Hellen for taking care of all things domestic while I was at school and for helping with the job of putting elastics on 1700 nails.

And lastly, I need to thank the physics community at the University of Toronto, especially Phil, Juan, and Ting for help with things theoretical, Ramin for discussions on scaling of Fourier transforms, Peter for LabView advice, and Antony for moral support. But mostly to Stephen Morris for picking an oddball case and providing her with every opportunity to succeed.

Contents

1 Introduction **1**

1.1 Background and Motivation 2

2 Experiment **7**

2.1 Experimental Setup 7

2.2 Experimental Procedure 12

2.3 Data Analysis Methods 14

3 Results and Discussion **23**

3.1 Visual Analysis 23

3.2 Computer Analysis 29

4 Conclusion **32**

References **33**

List of Figures

1.1 Illustration of particle alignment in nematic, smectic, and antiferromagnetic phases. 5

2.1 Details of the shaker plate. 9
2.2 Shaker apparatus 10
2.3 Closest packing experiment 13
2.4 Visually detected nail states 16
2.5 Examples of nail detection methods 18
2.6 Nematic order parameter analysis 20
2.7 Example of the line drawing method 21

3.1 Sample oscilloscope trace 24
3.2 Phase diagrams 26
3.2 Phase diagrams cont'd 27
3.3 Antiferromagnetic images as a function of time 30

Chapter 1

Introduction

In science classes students are often told that physics is the study of "energy and matter", a broad definition indeed. They are taught classical physics almost as a history lesson and as a foundation for greater things. But the discovery and development of modern physics has not ended enquiry into the properties of classical systems. There are still many interesting unanswered questions about energy and matter on the nonquantum, nonrelativisitc scale.

Many of the classical questions which still need answers are complex due to their nonlinearity. In linear systems, if there exist solutions to a set of equations, then any linear superposition of these is also a solution. But many systems in nature do not behave in this way, at least not under certain conditions. For example, the Navier-Stokes equations of fluid dynamics were developed in the 19th century, but still have limited analytic solutions due to their nonlinear behaviour in large areas of parameter space.

Pattern formation is another area where complexity can be found in a nonlinear classical system. Aranson and Tsimring [1] describe it loosely as, "a dynamical process leading to the spontaneous emergence of a nontrivial spatially nonuniform structure which is weakly dependent on initial conditions." Generally, pattern formation occurs in a nonequlibirum dissipative dynamical system driven to a point where it undergoes a

symmetry breaking instability to reach a patterned state. [2] Evidence of these patterns can be found in many materials, in any state of matter.

In this project we will discuss pattern formation in mechanically agitated granular materials. In particular, our system is comprised of vertically vibrated nail-shaped particles which are free to move in three dimensions. We report the observation of nematic, smectic, and antiferromagnetic order in this system as well as aggregate lateral movement we term as *heaping*. We obtain phase diagrams for the observed patterns as a function of the signal driving voltage and the packing fraction of the rods for two different aspect ratios. We outline our manual and semi-automated methods for determining the particle position and orientation and how these were used to calculate the nematic and antiferromagnetic order parameters. The results of initial investigations into nematic and antiferromagnetic ordering as a function of time and signal driving voltage using these methods are reported. We find that the higher aspect ratio particles tend to transition from random, through nematic, to smectic phases with increased packing fraction or decreased driving voltage. The lower aspect ratio particles tend to transition from random, through nematic, to either heaping or antiferromagnetic phases with increased packing fraction or decreased driving voltage.

In the remainder of the introduction, background into the study of granular materials will be given. Included are motivations of our choice of particle shape, terminology, and order parameters.

1.1 Background and Motivation

Composed of solid macroscopic particles, granular materials cannot be easily classified into one of the four traditional states of matter. [3] A system of granular material is out of equilbrium by its very nature. [4] The interactions between the particles are rapidly dissipative and thermal energy plays little role in the dynamics, so without a continuous

supply of mechanical energy the particles come to rest out of their potential mimina. [4] In systems where thermal energy is large enough to play a role in dynamics, anisotropic particles are known to form ordered states upon reaching thermodynamic equilibrium through the process of entropy maximization. [5]

Although they are not thermal systems, the behaviour of granular materials under weak mechanical agitation has been explored by others as an analogy to out-of-equilibrium thermal systems in order to understand the role of particle anisotropy in pattern formation. [5, 6] The analogy between the relaxation of shaken granular materials and the slow dynamics of out-of-equilibrium thermal system is based on the assumption that particle geometry is the most important parameter in the system. [6] Better definition of the role of shape on the ordering of systems of macroscopic particles and how it compares with other factors such as interparticle and external forces would be useful in furthering understanding of self-ordered systems, from the lipids and proteins of the cell membrane to the packing of pills and agricultural grains.

A review of the literature reveals that spherical [4, 7–10] and rod-shaped [5, 6, 11–15] particles have been the most commonly used for vibration studies. Although rods with tapered ends have been studied in a vertically-vibrated ensemble by Narayan et al. [16], we have not found any comparable investigation into the behaviour of particles that have a similar anisotropy as the ones chosen here. Our particles are rod-shaped, but terminated at one end by a short head with a diameter larger than their cylindrical body. As compared to rods, the nail head hinders a degree of freedom of movement; therefore, one particle cannot slide freely past its neighbor if it is lying closely parallel. This choice of particle shape was motivated by the expectation to see anitferromagnetic ordering, which has not been previously reported.

Rods are one of several highly anisotropic molecule shapes known to form liquid crystal phases. As our particles are modified rods, in order to describe the behaviour of the system under various conditions, terminology and concepts from the field of liquid

crystals and condensed matter physics were used. These will now be explained in detail.

An order parameter is a dimensionless number used to represent the amount of particle organization. 0 represents complete disorder and 1 represents perfect order. Of interest in this system are the nematic, smectic, and antiferromagnetic order parameters.

If the particles in a liquid, which by nature have no positional order, have anisotropic orientational order, it is known as a nematic phase. [17] Fig. 1.1a on the following page [18] illustrates the loss of rotational symmetry as the anisotropic molecules in a nematic liquid crystal lie with their long axis in the same general direction, the director **n**. In the nematic phase, **n** and $-\mathbf{n}$ are indistinguishable. [17] As explained in Chandrasekhar [19], in a 3-dimensional system of cylindrically symmetric rods, the nematic order parameter s is given by

$$s = \frac{1}{2}\left\langle 3cos^2\theta - 1 \right\rangle$$

where θ is the angle the long axis each rod makes with **n**. For particles which are not cylindrically symmetric, it is more valid to write s as a traceless tensor order parameter

$$s_{ij}^{\alpha\alpha} = \frac{1}{2}\left\langle 3i_\alpha j_\beta - \delta_{\alpha\beta}\delta_{ij} \right\rangle$$

where α and β refer to the Cartesian axes of space and i and j refer to the principle axes of the particle. i_α refers to the projection of the unit vector **i** along α. In the 2-dimensional system of this experiment, this was rewritten as[20]

$$s_{\alpha\beta} = \frac{1}{N}\sum_i \left(i_\alpha i_\beta - \frac{1}{2}\delta_{\alpha\beta} \right) \tag{1.1}$$

Liquid crystals in the smectic phase have orientational order plus positional order in one or two of the three spatial dimensions. This causes them to form stacked layers with well defined spacing, [17] as illustrated in Fig. 1.1b on the next page. [21] This layering creates a spatial density wave and the smectic order parameter, σ, measures its

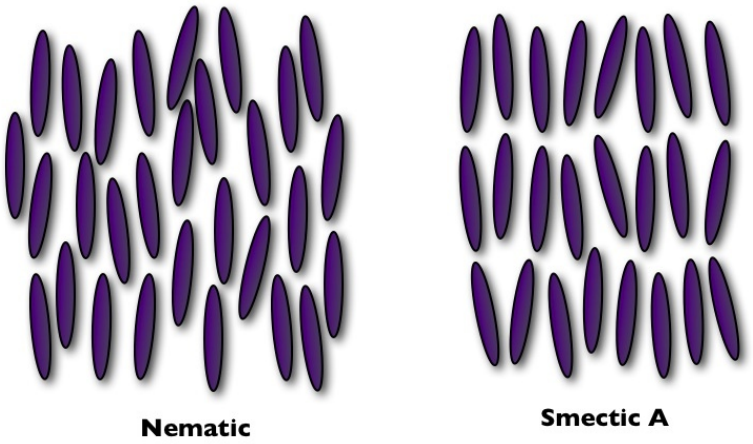

(a) (b)

(c) Antiferromagnetic

Figure 1.1: Illustration of particle alignment in nematic, smectic, and antiferromagnetic phases.

amplitude. In three dimensions,

$$\sigma = \left\langle cos(2\pi z/d)\left(\frac{3cos^2\theta - 1}{2}\right)\right\rangle \tag{1.2}$$

where z is the distance of the center of mass of a particle from the plane formed by the center of the layer and d is the layer thickness. [19] This order parameter expresses the dependence of smectic order on both the position of the center of masses and the orientation of the particles within the layer.

In an antiferromagnetic material, the magnetic moments of neighboring atoms or molecules align in an alternating pattern as shown in Fig. 1.1c. Athough the particles of this study were not magnetic, it was possible to assign a direction to the long axis of

each nail, as the ends are not interchangeable. In our analogy, the alternating head tail order corresponded to the alternating magnetic moments of an antiferromagnetic. The antiferromagnetic order parameter, ϕ, was defined as [22]

$$\phi = -\frac{1}{2N}\sum_{i,j}(i_\alpha j_\alpha + i_\beta j_\beta) \tag{1.3}$$

where i and j are adjoining particles. Again, α and β refer to the Cartesian axes of space, i and j refer to the principle axes of the particle, and i_α refers to the projection of the unit vector $\mathbf{i}$ along α. This parameter has a value of 1 for a pattern of alternating neighbors, 0 for neighbors of random orientation, and -1 for neighbors aligned in the same direction.

Having introduced our experiment, including background and motivation, the next section will outline the experiment including the experimental setup, experimental methods, and image analysis methods. The results and discussion will then follow. We will summarize the project and possible future direction in the conclusion.

Chapter 2

Experiment

The experiment consisted of analyzing the ordering behaviour of brass escutcheon pins, for simplicity referred to as nails, vibrated vertically on an aluminum plate. The vibration was controlled by an amplified signal generator input to an electromagnetic shaker. Aspect ratio, driving voltage, packing fraction, and shake time were varied. Accelerometer readings and high resolution images of the resulting nail arrangement were taken at regular intervals. This chapter details the experimental setup, experimental procedure and image analysis methods.

2.1 Experimental Setup

In this section we will give detailed information about the physical setup of the experiment. Information about the nails, the shaker plate and apparatus, as well as the lighting and image acquisition are presented.

Two sizes of nails were chosen in order to investigate the role of aspect ratio on ordering. The 1/2 inch #14 nails had a total length of approximately 1.46 cm and a head width of 0.432 cm giving an aspect ratio of 3.38. The 1 inch #18 nails had a total length of 2.67 cm and a head width of 0.254 cm to give an aspect ratio of 10.5. Individual nail masses were on average 0.450 g and 0.295 g respectively.

The 1 inch nails had a packing ratio of 0.808 g/cm^2, which meant that to have 100% packing fraction on the 645 cm^2 plate would require 521 g of nails. The 1/2 inch nails had a packing ratio of 1.33 g/cm^2, which meant that 100% packing would require 858 g of nails.

The shaker uses an electromagnet with a strong magnetic field. Brass nails were chosen so the dynamics of the grains would not be affected by this field. To aid with image analysis, two dental elastics, one blue the other green, were placed on the nail just below the head. Further details of their purpose will be given in Section 2.3 beginning at page 17.

A 10 inch by 10 inch square (645 cm^2), aluminum shaker plate was designed for this experiment. Design considerations balanced the need for minimal mass to reduce the demand on the shaker and rigidity to prevent the formation of nodes of vibration; see Fig. 2.1a on the next page. Four clear plexiglass walls attached around the outer edge contained the nails to the plate without obstructing observation and lighting from the side. A removable plexiglass barrier was created to create a smaller plate area when needed.

The plate was created to attach to the shaker by one of two coupling mechanisms, a circular cone or a square plate used in conjunction with a linear air bearing. The shaker leveling mechanism was improved so the experiments could be run with the plate directly connected to the shaker via the circular cone, as shown in Fig. 2.1b on the following page.

The frequency and amplitude of vibration for the shaker were driven by an Agilent 33120A frequency generator signal passed through a Crown CE 1000 amplifier. The acceleration of the plate was a result of not only the driving signal but also the impact of the nails upon its surface. To measure the acceleration of the plate, a PCB Piezoelectronics XYZ-accelerometer model 356B06 was attached to its underside at its center. The detected signal was passed through a PCB Piezoelectronics sensor signal conditioner and the Z and Y components were read by a Tektronix TDS210 two-channel oscilloscope

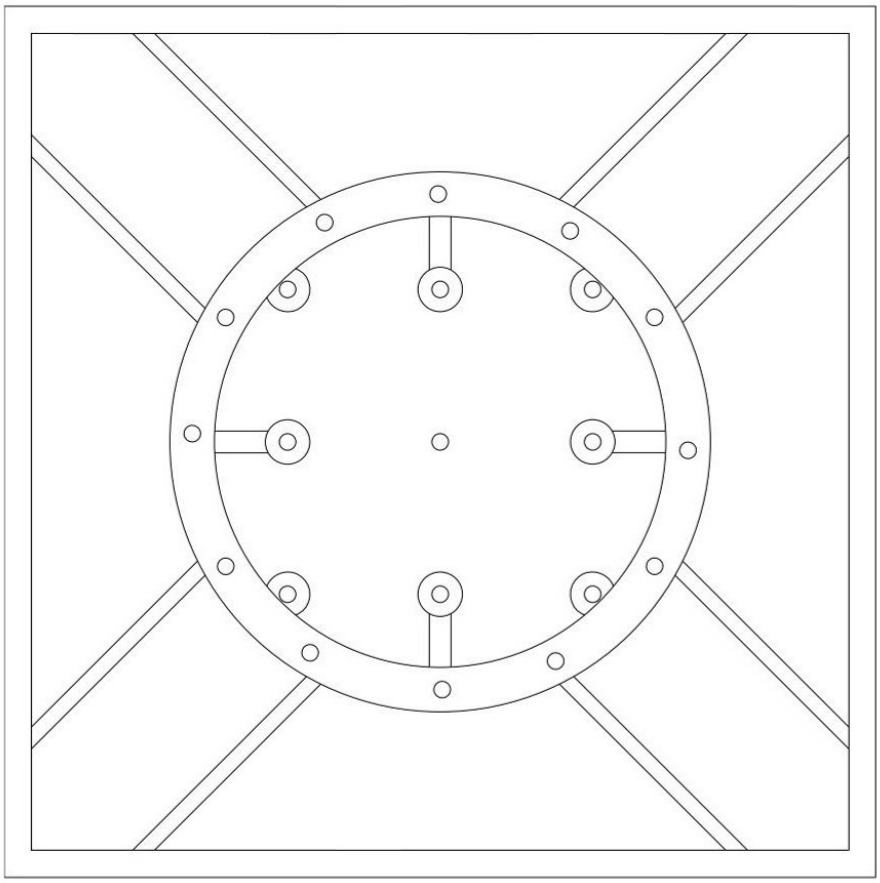

(a) Design of the underside of the shaker plate.

(b) Side view of the shaker plate, showing the barrier walls and circular cone.

Figure 2.1: Details of the shaker plate.

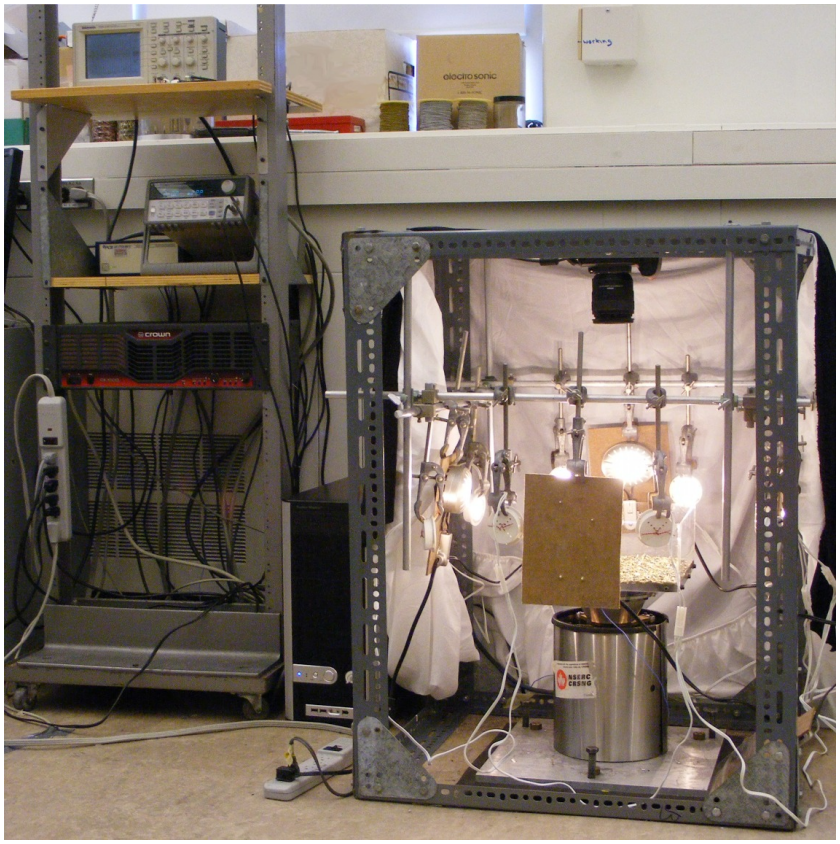

Photograph

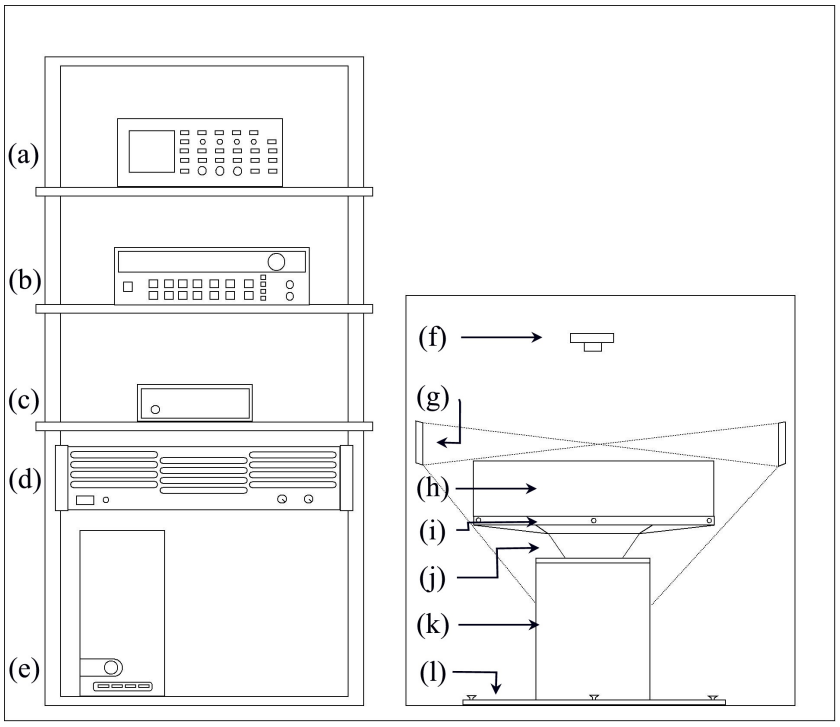

Diagram

Figure 2.2: Shaker apparatus as explained in text: (a) oscilloscope (b) signal generator (c) signal conditioner (d) amplifier (e) computer CPU (f) camera (g) light sources (h) plexiglass barrier (i) shaker plate (j) adapter cone, containing the accelerometer (not shown) (k) shaker (l) leveling plate

using the frequency generator signal for triggering. Due to the varied nature of the amplitude with time, 128 trace signal averaging was used. LabView code was written to give the option of automation of both the output of the signal generator and the capturing of the oscilloscope measurements and associated images. A photograph and diagram of the apparatus, including lighting and camera, are shown in Fig. 2.2 on the previous page.

Images were taken with a Nikon D70S camera attached at a fixed distance from the surface of the plate. Image acquisition was triggered via LabView code. The 3008x2000-pixel uncompressed NikonRAW images were stored on the camera and transferred to the computer after an experimental run. They were then either converted directly to uncompressed 16-bit RGB-tiff files for analysis or underwent a histogram adjustment using NikonEditor software before conversion, depending on the analysis being done. The quality and consistency of the images before conversion were of great importance for automated analysis. To aid in this, the aluminum plate was painted black so that the nails would contrast with it well and to remove from the images a reflection of the camera above. The flash setting could not be used as it created bright spots on the plate and intense reflection from the nails. Four to twelve xenon and halogen lamps were wired and arranged so that their beams would be obliquely incident upon the nails in order to remedy this. As the ambient light in the room changed throughout the day, the whole experiment was draped with a layer of white cloth to diffusely reflect stray light back toward the experiment and a layer of black cloth to block external light.

It was noted that the nails colliding with the plate wore and chipped the black paint. This resulted in a darkening of both the nails and the elastics, which made the semi-automated image analysis more difficult. The nails had to be cleaned between each change of packing fraction in order to keep the colors consistent. Some method of either protecting the painted surface, like covering the plate in a sheet of plexiglass, or anodization needs to be considered; although anodization may not be durable against damage by the nails. Another option might be to consider shaking plastic forms color tagged in

some fashion, which would be lighter and should do less damage.

2.2 Experimental Procedure

Now that the apparatus has been explained, we will give details of the experimental procedure. Motivations for choices of parameters are given as well as what data was obtained.

It was decided to select a single frequency at which to experiment in order to eliminate any changes in the shaker leveling that might occur at different frequencies. Trial runs were used to determine which area of parameter space to explore.

In the first of two experiments with 1 inch #18 nails, runs were taken at a fixed frequency of 37.0 Hz, starting with a mass of nails on the plate of 204.4 g and increasing the mass by approximately 20.5 g, up to a mass of 409.8 g. For each mass, the amplitude at the frequency generator was varied from 400 mVPP to 180 mVPP and returning to 400 mVPP in steps of 20 mVPP. A step was made every 120 seconds, with 3 oscilloscope measurements and images taken per step. The results of this experiment were used to create a phase diagram using visual analysis, which will be explained in the following section.

From observing smectic layers in the 1 inch #18 nail system, in the second experiment with this nail length, it was decided to investigate the behaviour of these layers with time. Analogous to a crystal, the nails were laid on the plate in closest packing formation with alternating head-tail orientation into full layers. The removable plexiglass barrier was inserted to keep the nails constrained to the area covered by this monolayer, which was 389.8 g on 80.7% of the surface. To "melt" the crystal, the driving voltage was increased incrementally. A video was created of the behaviour of the nails as the driving voltage was increased at regular intervals, approximately 5.0 mVpp every 2 minutes. Still images were captured at every 30 seconds; samples of these are shown in Fig. 2.3 on page 13.

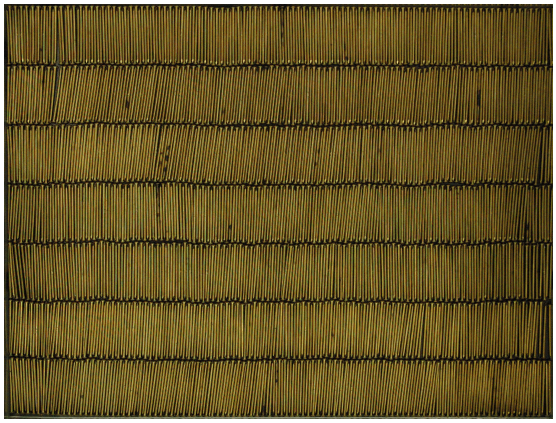

(a) Nails before shaking.

(b) Layers beginning to tilt.

(c) Introduction of defects.

(d) Movement of layers.

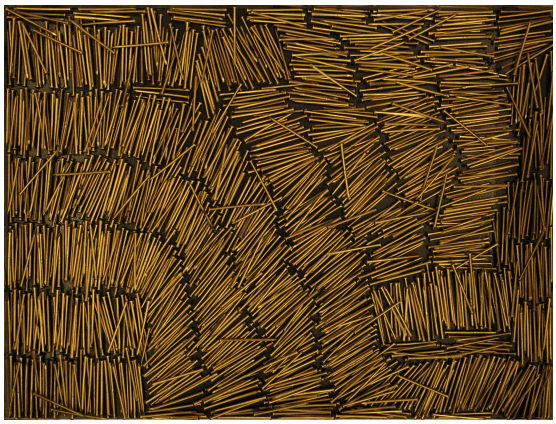

(e) Movement of layers.

(f) Nematic, but layers still visible.

Figure 2.3: Examples of the closest packing experiment with 1 inch nails as outlined in the text. Images are cropped to show the area of the plate covered by the monolayer. (a) 0 minutes, 0 mVpp (b) 5 minutes, 170 mVpp (c) 22 minutes, 230 mVpp (d) 36 minutes, 280 mVpp (e) 49 minutes, 305 mVpp (f) 102 minutes, 540 mVpp

This video showed the movement of the layers and the creation and movement of defects with time. It also showed the transition from smectic to nematic phases in a high-density monolayer.

In the first of two experiments with 1/2 inch #14 nails, runs were taken at a fixed frequency of 37.0 Hz, starting with a mass of nails on the plate of 410.6 g and increasing the mass by approximately 40.6 g, up to a mass of 821.3 g. For masses in the range 410.6 g to 694.9 g, the amplitude at the frequency generator was varied from 400 mVPP to 180 mVPP and returning to 400 mVPP in steps of 20 mVPP. As the mass increased, the nails began to heap at low driving voltages, so the input voltages were adjusted as shown in Table 2.1. A step was made every 120 seconds, with 3 oscilloscope measurements and images taken per step. A phase diagram was also created for this experiment using visual analysis of the images obtained.

As the amount of antiferromagnetic ordering that had been observed previously during experimental setup was not displayed over at least half the plate during this experiment, it was decided to determine if time was a factor in the amount of antiferromagnetic ordering. Runs were done with 821.3 g of 1/2 inch #14 nails shaken at 220, 240, 260, and 280 mVpp with oscilloscope measurements and pictures taken every minute for five minutes.

Table 2.1: Driving voltage for masses of 1/2 inch nails during the first of two experiments with this length outlined in the text.

Mass (g)	Driving Voltage Range Descending (mVpp)	Driving Voltage Range Ascending (mVpp)
410.6 - 694.9	400-180	180-400
735.6	400-180	220-400
776.4	220-440	460-240
821.3	260-480	480-260

2.3 Data Analysis Methods

Initial runs with the 1 inch #18 nails showed that automated extraction of numerical data from the resulting images would be unyielding as overlapping nails made it impossible to use common methods of image analysis to define single particles within the image. Visual analysis was used to categorize each picture using a definition of each state. A time-intensive manual detection method was created to find the center and orientation of each nail, as shown in Fig. 2.5a on page 18. A semi-automated method of color tagging using blue and green dental elastics allowed for the detection of individual nails and their orientation. Once the position and orientation of the nails were determined, nematic and antiferromagnetic order parameters were calculated. This section details each of these methods.

In the visual detection method, photographs were visually inspected and catagorized as one of: random, nematic, smectic, antiferromagnetic, heaping, or other, as follows:

random Particles show no order.

nematic Particles show orientational order. Observed groups of a minimum of 5 to 10 nails oriented in the same general direction. No consideration of the direction of their individual heads or the relative positions of their center of masses.

smectic Particles show orientational and positional order. Observed groups of a minimum of 5 to 10 nails oriented in the same general direction forming a density wave with at least two "crests". Centers not misaligned by more than what was judged to be 1/8 of the length of the nail excluding the head. No consideration of the direction of their individual heads.

antiferromagnetic Particles show orientational and positional order. Observed groups of a minimum of 5 nails oriented in the same general direction, with an alternating position of their head. Centers not misaligned by more than what was judged to be 1/8 of the length of the nail excluding the head. No consideration to number of "crests" in the density wave.

heaping Particles move in unison in a particular direction, causing them to pile.

other Any unexpected phase.

A photograph was not characterized as being in the category unless approximately half the image was in that state. Fig. 2.4 on the next page shows examples of nails in various states. This method was subjective and although care was taken to be as objective as possible, numerical methods of calculating the order parameters were created to limit this subjectivity. These will be explained next.

A manual nail detection MATLAB script was written that calculated the position of the center of the nail and its orientation based on the selection of the head and then the tail of each nail by the user. Fig. 2.5a on the following page shows an example of the results. This method was very accurate, as 100% of the nails could be marked to within 3°, but it was very time-consuming.

To reduce the time taken to analyze a picture, the 1/2 inch nails were tagged with two dental elastics, green and blue. This was only possible for the 1/2 inch #14 nails, because the heads of the 1 inch #18 nails were so small in diameter that the elastics would have touched the plate. To extract information from images of tagged nails, MATLAB code [23] was written that determined the pixels corresponding to individual blue and green elastics. Given the RGB values corresponding to numerous shades of blue and green in the picture, the color distance, ΔC, of each pixel from each of the given color shades was determined using the formula [24]

$$\bar{r} = \frac{C_{1,R} + C_{2,R}}{2}$$

$$\Delta R = C_{1,R} - C_{2,R}$$

$$\Delta G = C_{1,G} - C_{2,G}$$

$$\Delta B = C_{1,B} - C_{2,B}$$

$$\Delta C = \sqrt{\left(2 + \frac{\bar{r}}{256}\right) \times \Delta R^2 + 4 \times \Delta G^2 + \left(2 + \frac{255 - \bar{r}}{256}\right) \times \Delta B^2} \tag{2.1}$$

(a) Example of leaving random and becoming nematic.

(b) Example of nematic, approaching smectic.

(c) Example of leaving nematic and becoming smectic.

(d) Example of approaching antiferromagnetic.

(e) Example of antiferromagnetic.

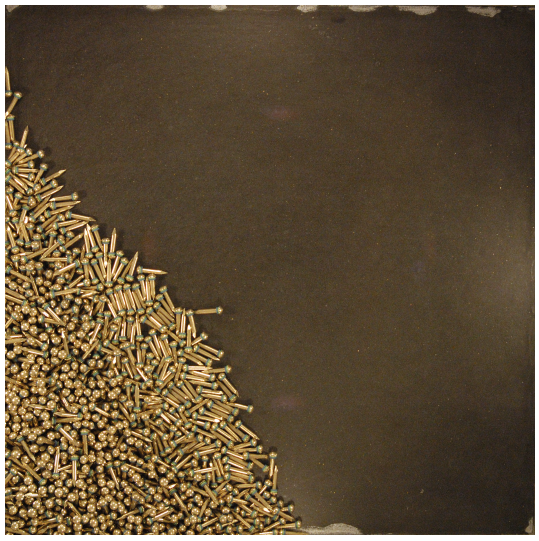

(f) Example of heaping.

Figure 2.4: Examples of the various visually detected nail states. (a)-(c) show 1 inch #18 nails. (d)-(f) show 1/2 inch #14 nails. Images show the full area of the plate.

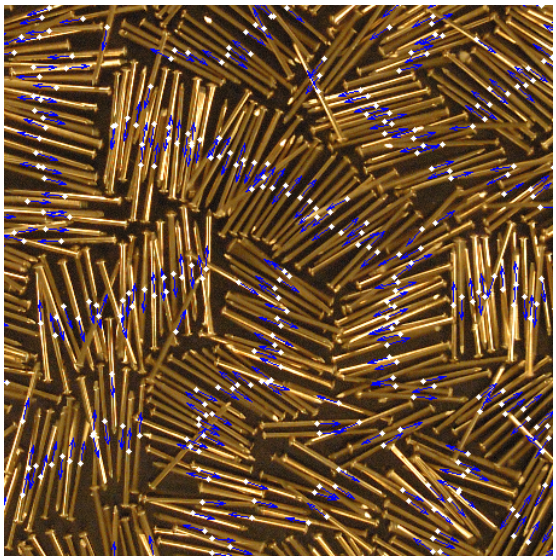

(a) Nails that have been manually detected.

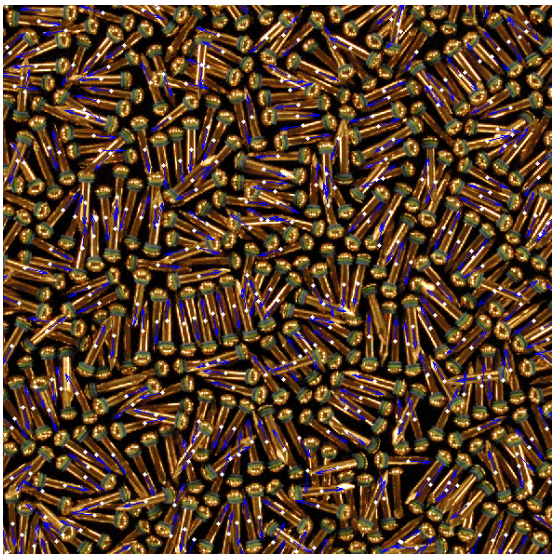

(b) Nails that have been detected using tagging, before editing.

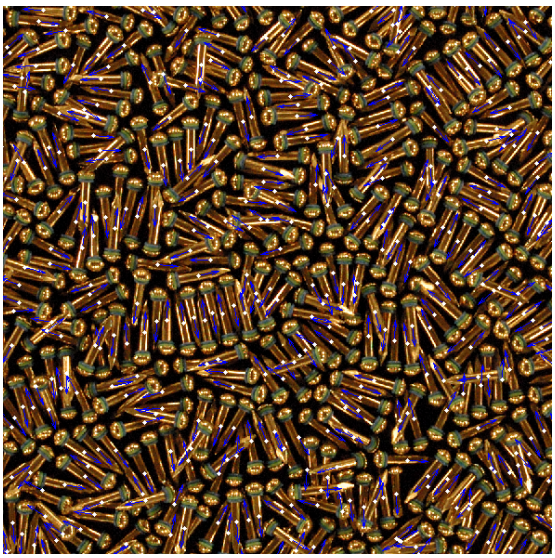

(c) Nails that have been detected using tagging, after first edit.

Figure 2.5: Examples of the results of the detection methods outlined in the text. Images are cropped to 1/4 of the plate area in order to show detail.

where $\bar{r}$ is the average of the red layer of the image, ΔR is the difference between the red value of the pixel and the red value of that shade, ΔG is the difference between the green value of the pixel and the green value of that shade, and ΔB is the difference between the blue value of the pixel and the blue value of that shade. If the distance between a pixel and a shade was below a certain threshold, it was considered to be that color.

A mask layer for each color was created by setting any pixel determined to be blue or green to white in that particular mask while leaving all other pixels black. Image erosion and dilation were performed and then areas which were too small or too large to be a single elastic were discarded. The centers of the blobs corresponding to the elastics were found. A line was fit through the area corresponding to each blue elastic, and from its angle the angle of the long axis of its nail was calculated. The position the center of the nearest-neighbor green elastic, found through Delaunay triangulation, was used to determine the correct head-tail orientation of the nail. Using a typical number of pixels from the center of the blue elastic to a nail center and the calculated angle, the position of the nail center was determined. The automated results were then edited by deleting the incorrect nail data and marking the deleted and missing ones. The editing was repeated until it was felt that 90% of the nails were marked to within 3°.

Now that we have explained how the angle and position of each nail was determined, we will explain which order parameters were calculated and what methods were used to do so.

To determine the nematic order parameter, s, MATLAB code was written that calculated the tensor order parameter given in Eq. 1.1 on page 4 for square areas with length three times that of a nail meshed over the surface of the plate. This meshing was done to account for the changes in orientation of the director over different regions of the plate. The value of s for each area was calculated as the two times the length of the largest eigenvalue of its tensor order parameter. The factor of two was necessary to normalize the value of s, following the discussion of Eppenga and Frenkel [25]. Areas enclosing

(a) A visual representation of the meshing process.

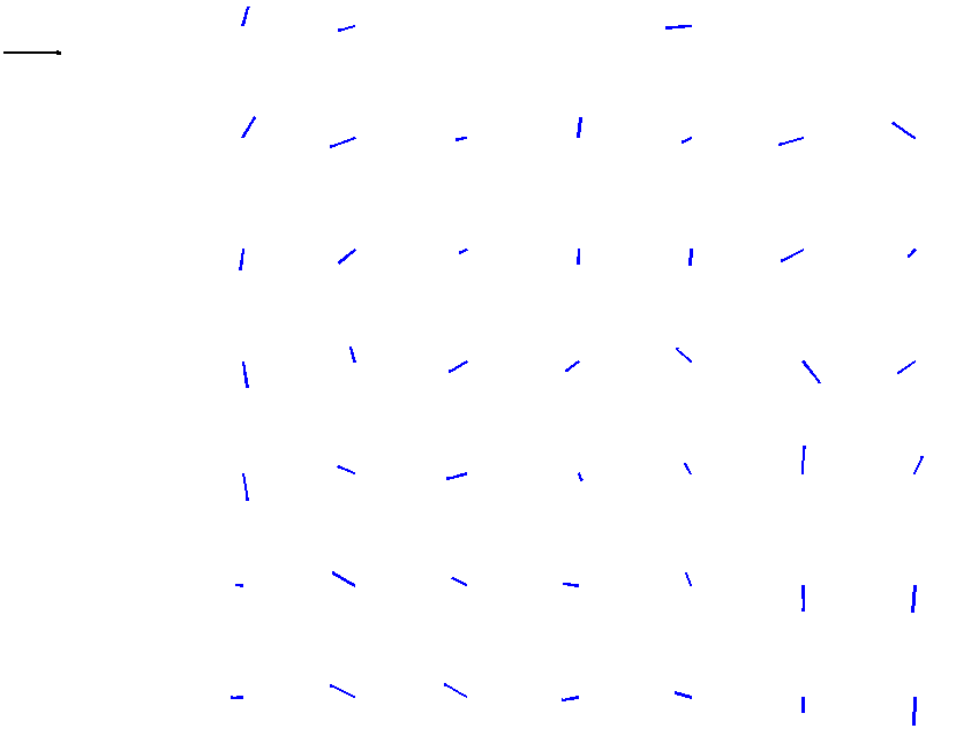

(b) A visual representation of the resulting directors for each mesh. Each director is scaled by a factor of the nematic order parameter in that area. The black vector in the top-left represents unity.

Figure 2.6: Illustration of the process and results of the nematic order parameter analysis.

fewer than ten nails were not considered as the parameter is based on a statistic average. Fig. 2.6 on the next page illustrates the meshing process and displays the resulting directors scaled by the length of the nematic order parameter.

In order to determine the smectic order parameter, σ, as described in Eq. 1.2 on page 5, a line drawing method to create an image to represent any possible density waves in the data was created. To do this, lines were drawn from each nail center to its two nearest neighbors on either side of a line drawn through the nail on its long axis. Only nails within a distance of three times the width of a nail were considered for the nearest neighbor algorithm, which used a Euclidean distance metric. [26] Figure 2.7 shows a sample result. More work is needed to numerically represent this as an order parameter.

To determine the antiferromagnetic order parameter, ϕ, MATLAB code was written to perform the calculation of Eq. 1.3 on page 6. Using the same nearest neighbor algorithm as for the smectic line drawing, the two nearest neighbors on either side of a line drawn through each nail on its long axis were found. Again, neighbors had to be within a distance of three times the width of a nail, called the neighborhood. The dot product of a nail with its neighbor was performed, and then this result was multiplied by a weighting function which had a value of one for half the width of the neighborhood and tapered Gaussian slope to the edge of the neighborhood. These values were summed over the image and normalized by the number of neighbors.

Using these methods and procedures we extracted the degree of order as a function of driving voltage and packing fraction for two different aspect ratios. We observed the dynamics of a closest packing arrangement for the 1 inch # 18 nails with increases in driving voltage over time. We also determined the degree of order as a function of driving voltage and time for the 1/2 inch # 14 nails. In the next section we will present and discuss the results of the experiments.

(a) Nail image

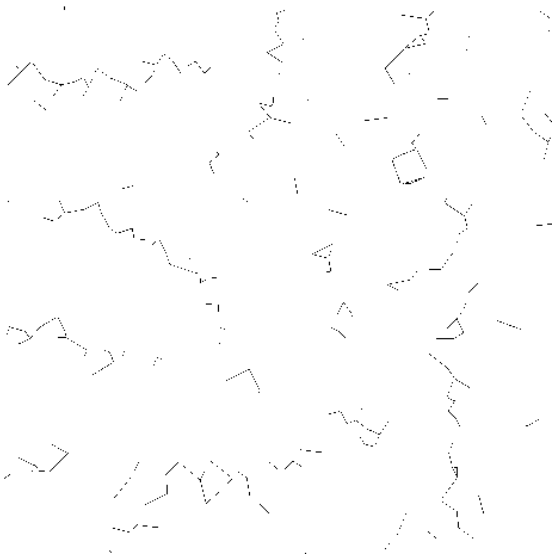

(b) A visual representation of the resulting lines drawn between the neighboring nails.

Figure 2.7: Example of the results of the line drawing method outlined in the text. Images are cropped to 1/4 of the plate area in order to show detail.

Chapter 3

Results and Discussion

In the first section, our project was outlined and background was given. In the previous section, experimental equipment, experimental methods, and data analysis methods were presented. In this section we will give the results of the experiments and discuss their significance. We will consider first the results of the visual analysis, namely the phase diagrams for each size nail and the results closest packing experiment and then the computer analysis of the nematic and antiferromagnetic order parameters.

3.1 Visual Analysis

Measurements from the accelerometer output to the oscilloscope were analyzed in order to determine the acceleration for each driving voltage. Even with 128-trace signal averaging, the amplitude of acceleration as a function of time appeared noisy. This would indicate that the effect of the nail collisions with the plate was not completely random, as signal averaging amplifies a weak signal while reducing random noise. For each image, the corresponding oscilloscope traces were smoothed and the peaks were detected. [27] An example is shown in Fig. 3.1 on the following page. From these peaks, an average acceleration for each image acquisition was calculated. Plotting these accelerations versus driving voltage showed that the resulting acceleration was not linear with the sinusoidal

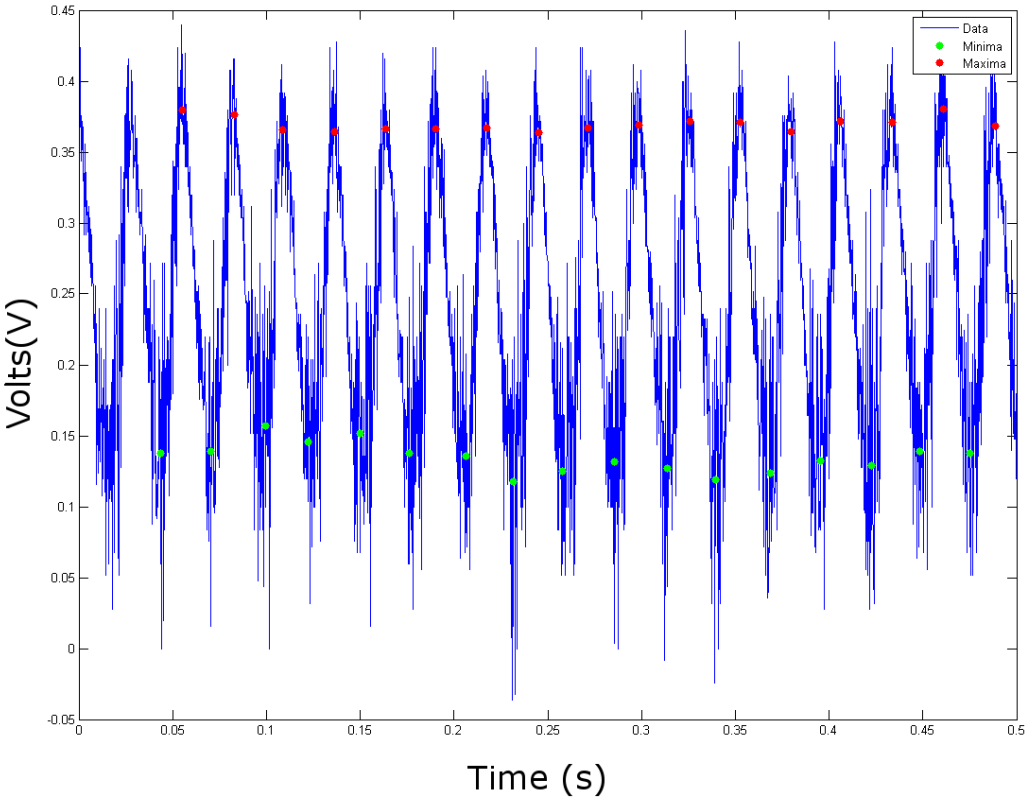

Figure 3.1: A sample image of an oscilloscope trace. The peaks detected on the smoothed data are indicated.

driving signal.

Further analysis of the behaviour of the plate was performed. While vibrating equivalent masses of water at the same driving voltages, this wide acceleration variation was not present and the resulting accelerations had a direct correlation with the driving voltages. This supports the supposition that the variation is due to the collisions of the nails with the plate. To overcome the effect of the nails on the plate would require a significant change in the apparatus design, such as increasing the mass of the plate and the strength of the shaker in order to reduce the effect the nails had on the plate's acceleration, shaking lighter objects for the same purpose, or creating LabView code to use the accelerometer readings to create a feedback mechanism in order to keep the vertical motion of the plate versus time sinusoidal. The use of a linear bearing to keep the plate

from vibrating horizontally or a lock-in amplifier on the accelerometer signal might also help. These modifications were beyond the scope of the current study. Because of this issue, phase diagrams were given as a function of driving voltage.

Through visual analysis of the data from the first experiments with each of the two nail lengths, the state of the nails for each picture was determined as outlined in Section 2.3. Resulting phase diagrams are shown in Fig. 3.2 on pages 26 and 27. Multiple points at the same x,y values on the diagram are plotted near to each other, so a larger area indicates more samples at those conditions.

Examining first the results for the 1 inch #18 nails on page 26, we observe changes in states of order. The nails went through random, nematic, and smectic ordering as the input voltage was decreased or as packing fraction increased. Antiferromagnetic ordering was not apparent. The head of these nails only overhangs the cylindrical shaft by 0.6 mm, so it may be that is not enough to stop the nails from sliding past their neighbors, at least at the packing fraction examined.

The results for the 1/2 inch #14 nails on page 27 show again changes in states of order. However, the transitions were from random to nematic to heaping. Head-tail ordering was apparent in a significant number of the nematic pictures, but not enough to account for half the plate area. There tended to be stripes of nematically-ordered nails in domains that were longer than they were high, but these domains did not form stacked layers so were not considered to be smectic.

According to Narayan et al. [16], equilibrium Monte Carlo studies show that an aspect ratio greater than 7 is needed to produce a two dimensional nematic. The 1 inch nails, having an aspect ratio of 10.5, clearly show nematic behaviour. Narayan et al. [16] also suspect that nematic order occurs with particles that have narrower tips than waists which allows them to interdigitate, as their rods showed no nematic behaviour. The particles of this experiment are not wider at the waist but at the end, yet nematic behaviour is clearly apparent.

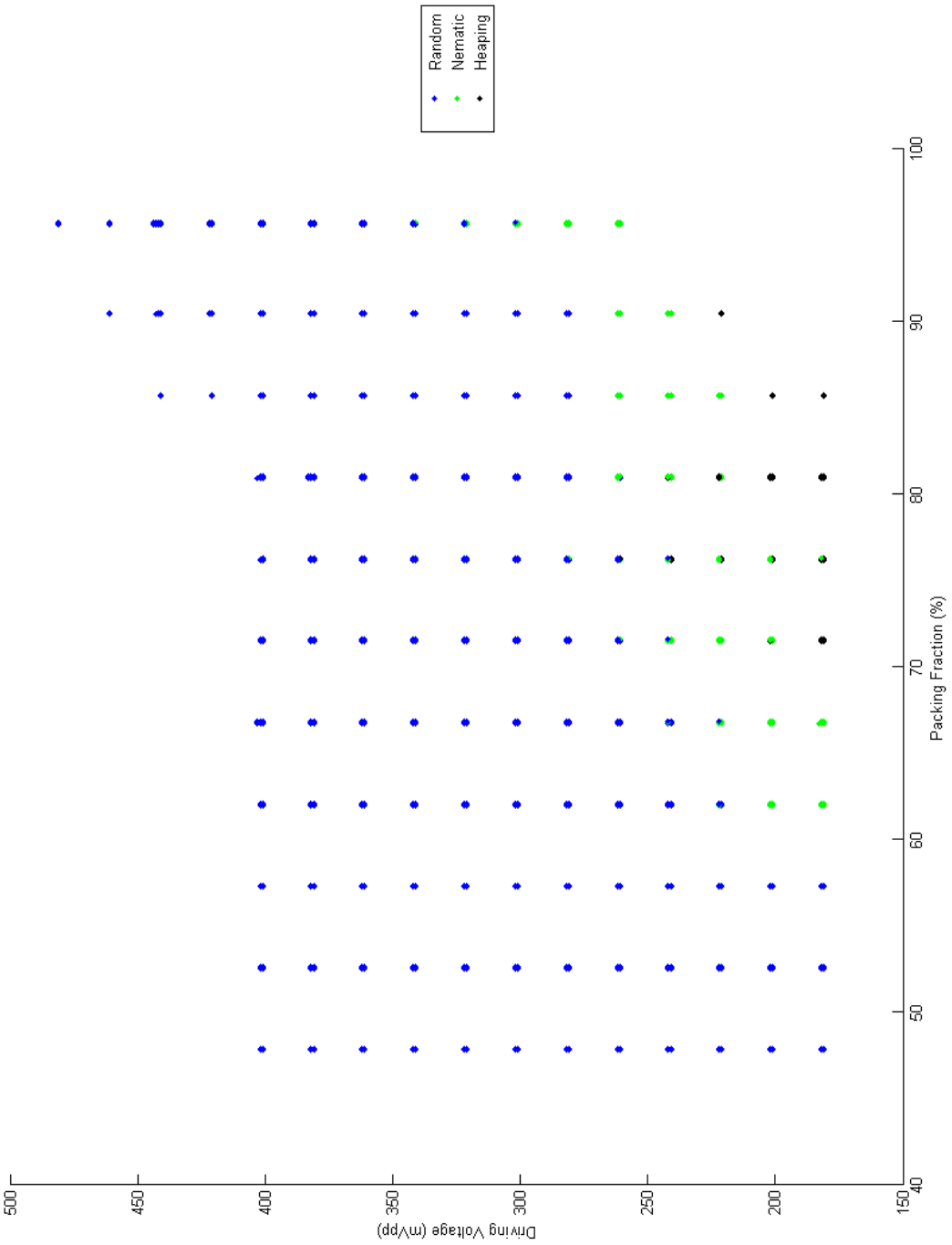

(a) 1 inch #18 nails phase diagram

Figure 3.2: Phase diagrams of driving voltage versus packing fraction.

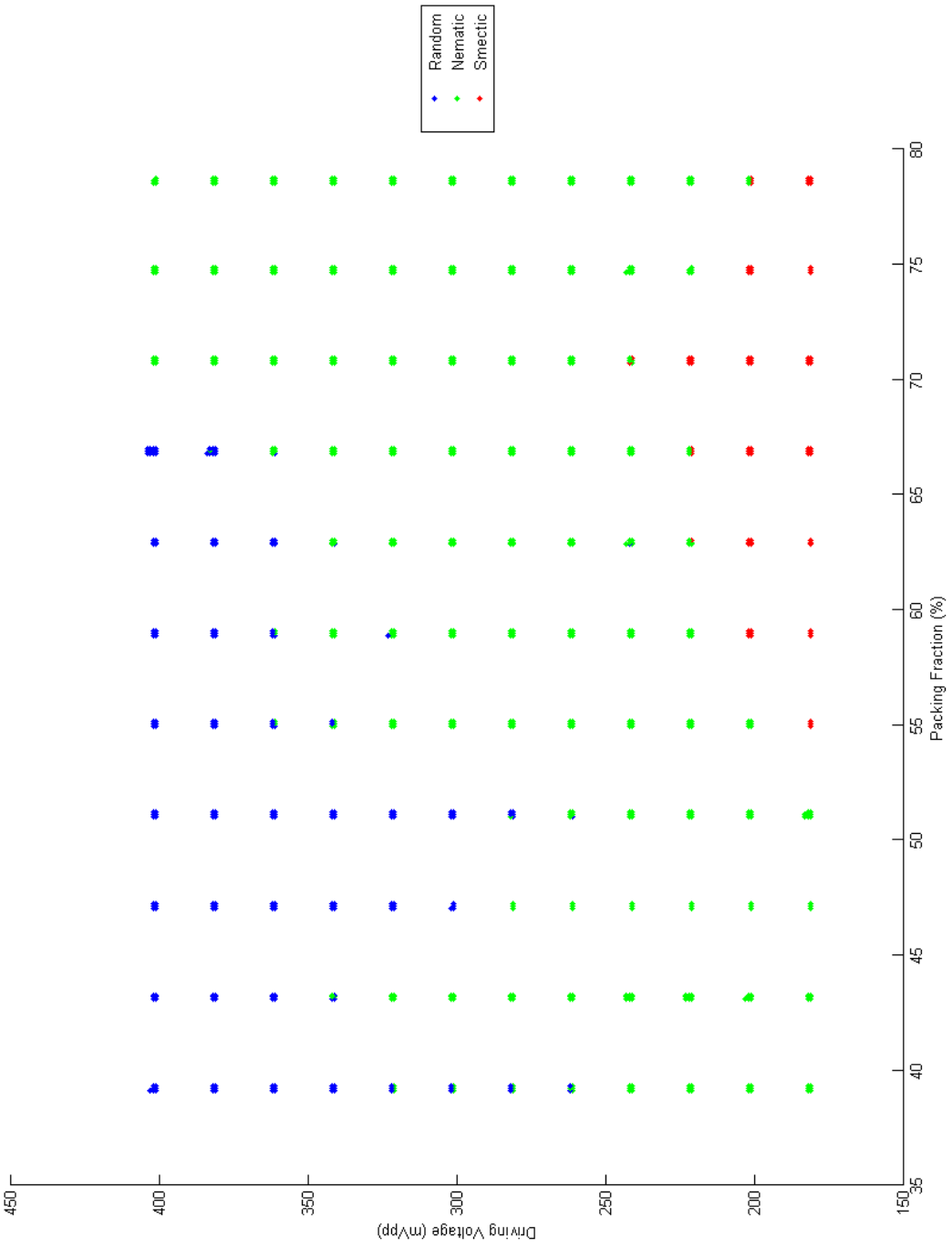

(b) 1/2 inch #18 nails phase diagram

Figure 3.2: Phase diagrams of driving voltage versus packing fraction cont'd.

The nematic behaviour of the 1/2 inch nails is arguable, as the domains considered were small. But it could also be that the aspect ratio should be calculated based on the length of the shaft of the nail versus its diameter instead of the length of the full nail versus the head diameter. This would give a an aspect ratio of 7.9 for the 1/2 inch nails and 25.2 for the 1 inch nails.

According to Narayan et al. [16], two-dimensional systems at thermal equilibrium have strictly short ranged smectic order. Although they observe smectic order in their system, they state that a large system in needed in order to differentiate if what was observed was a true long-range smectic which occurs because the system is not thermal, a weakly-ordered two-dimensional crystal, or a smectic that would become nematic on larger length scale. As the ratio of the length of the particles of this experiment to the diameter of their round shaker plate is of the same order of magnitude of the ratio of the length of the particles in this experiment to the width of the shaker plate, the same conclusion should probably be drawn.

The heaping behaviour of the 1/2 inch nails was interesting in that the nails moved as a unit. The direction of movement was not always the same. Experiments by Aranson et al. [13] "unambiguously identified the horizontal twisting component of the bottom plate oscillations as a primary source of overall collective grain motion." Further study is needed to understand why in our system collective movement leads to heaping rather than the swirling observed in their system.

The "crystal" formed by placing the 1 inch nails in perfect head-tail alternating alignment at 100% packing fraction proved to be very robust against vibration. The smectic ordering was still present at an input voltage of 300 mVpp. And although the centers of masses started to move out of alignment with the center of the layer by more than 1/8 of a nail-length just above that voltage, the layering was still visible over 400 mVpp.

3.2 Computer Analysis

As the manual marking of the nails was extremely laborious, only two images were processed in this fashion. They were both images 1 inch #18 nails at 67% percent packing fraction from the first experiment on these nails and in the smectic state, although one had more smectic order than the other under visual inspection. It was hoped that they would show a difference in their smectic order parameter, σ, but as the algorithm written was unsuccessful, this cannot be verified. The value of their nematic and antiferromagnetic order parameters are reported in Table 3.1.

Images from the second experiment on the 1/2 inch #14 nails at 95.7% packing fraction at the input voltages of 220 mVpp, 240 mVpp, and 260 mVpp at 1 minute and 5 minutes were examined to see if there was any visually apparent change in ordering. It appears that there was little change in the images at 260 and 220 mVpp, and notable the 220 mVpp sample appeared to be in the antiferromagnetic state. The 240 mVpp image showed a slight amount of change, with some but not all areas that had nails aligned head to head shifting to head to tail. It was judged that the amount of nematic ordering was about the same for all three images. It is noteworthy that as a result of the issue of heaping in the first experiment, 220 mVpp at this packing fraction was not examined, but could now be placed on the phase diagram as antiferromagnetic at 1 minute. 240 mVpp was the lowest driving voltage of that run; at 1.5 minutes it was showing antiferromagnetic ordering, but not over half the area of the plate. Using the process of automated nail center and orientation detection combined with editing,

Picture Number	s	ϕ
5306	0.341	-0.00360
5312	0.341	-0.0730
random	0.192	-0.0174

Table 3.1: Nematic and antiferromagnetic order parameters for 1 inch #18 nails. Values for random data are given as a comparison.

(a) 260 mVpp 1 minute

(b) 260 mVpp 5 minutes

(c) 240 mVpp 1 minute

(d) 240 mVpp 5 minutes

(e) 220 mVpp 1 minute

(f) 220 mVpp 5 minutes

Figure 3.3: Examples of the experiment with 1/2 inch nails at 95.7% packing fraction to determine if time was a factor in antiferromagnetic ordering, as outlined in the text. Images are cropped to 1/4 of the plate area in order to show detail.

Driving Voltage (mVpp)	Time (minutes)	s	ϕ
260	1	0.292	0.137
260	5	0.229	0.158
240	1	0.282	0.128
240	5	0.301	0.215
220	1	0.287	0.292
220	5	0.280	0.315
random		0.192	-0.0174

Table 3.2: Summary of nematic (s) and antiferromagnetic (ϕ) order parameters at various driving voltages for 1/2 inch #14 nails at 95.7% packing fraction. Values for random data are given as a comparison.

followed by the computer analysis, values for the nematic and antiferromagnetic order parameters s and ϕ were found at each driving voltage and time. These are summarized in Table 3.2. This small data set indicates that while the nematic order parameter for these images is not much higher than that of a random sample and might increase or decrease, the antiferromagnetic order is much higher than that of a random sample and did increase with time. A larger dataset is required to confirm this finding.

Chapter 4

Conclusion

In summary, a study of pattern formation in vertically vibrated nails was presented. Using visual analysis, phase diagrams for head width:nail length aspect ratios of 3.38 and 10.5 have been drawn for packing fractions in the ranges of 48% to 96% and 39% to 79% respectively with driving voltages ranging from 180 mVpp to 400 mVpp and 180 mVpp to 480 mVpp. While the larger aspect-ratio nails show strong nematic ordering with smectic ordering, the smaller-aspect ratio nails show short range nematic ordering that with time at high packing fraction and low driving voltages develops into antiferromagnetic order. Collective lateral motion was also noted at high packing fraction and low driving voltage.

Methods have been developed that can semi-automatically extract the position and orientation of each nail and calculate the nematic and antiferromagnetic order parameters for the images. This was used to analyze a small dataset to show it is now be possible to systematically examine the effect of driving voltage, packing fraction and aspect ratio on the two order parameters, eliminating the judgement factor of the visual analysis.

Interesting future study could include the examination other values of the parameters of this report, namely driving voltage, packing fraction, aspect ratio, frequency, and time. Also, using a more powerful shaker to accelerate a plate with a much larger surface area would allow for studies to see if there is true long-range smectic ordering in this

two-dimensional system. Although a method to calculate the smectic order parameter remains to be developed, this would be of great interest because if found, it would be an example of where the analogy of macroscopic granular materials being a model system for microscopic thermal systems breaks down. The effect of the boundary on the behaviour of vertically vibrated nails could also be studied using plates of different shapes. These studies could lead to a better understanding of the role of particle shape on granular systems under mechanical agitation as compared to that for thermal systems near equilbrium.

References

[1] I.S. Aranson and L.S. Tsimring. Model of coarsening and vortex formation in vibrated granular rods. *Phys. Rev. E*, 67(2):02130, 2003.

[2] S.W. Morris. Experimental nonlinear physics group. URL `http://www.physics.utoronto.ca/ nonlin/index.html`.

[3] H.M. Jaeger and S.R. Nagel. Physics of the granular state. *Science*, 255(5051): 1523, 1992.

[4] A. Kudrolli. Size separation in vibrated granular matter. *Rep. Prog. Phys.*, 67:209, 2004.

[5] D.L. Blair, T. Neicu, and A. Kudrolli. Vortices in vibrated granular rods. *Phys. Rev. E*, 67(3):031303, 2003.

[6] P. Ribiere, P. Richard, D. Bideau, and R. Delannay. Experimental compaction of anisotropic granular media. *Eur. Phys. J. E.*, 16:415, 2005.

[7] P.K. Das and D. Blair. Phase boundaries in vertically vibrated granular materials. *Phys. Lett. A*, 242:326, 1998.

[8] I.S. Aranson, D. Blair, W.K. Kwok, G. Karapetrov, U. Welp, G.W. Crabtree, V.M. Vinokur, and L.S. Tsimring. Controlled dynamics of interfaces in a vibrated granular layer. *Phys. Rev. Lett.*, 82(4):731, 1999.

[9] P.B. Umbanhowar, F. Melo, and H.L. Swinney. Periodic, aperidic, and transient patterns in vibrated granular layers. *Physica A*, 249:1, 1998.

[10] P. Melby, F. Vega Reyes, A. Prevost, R. Robertson, P. Kumar, D.A. Egolf, and J.S. Urbach. The dynamics of thin vibrated granular layers. *J. Phys. Condens. Matt.*, 17:S2689, 2005.

[11] F.X. Villarruel, B.E. Lauderdale, D.M. Mueth, and H.M. Jaeger. Compaction of rods: Relaxation and ordering in vibrated, anisotropic granular material. *Phys. Rev. E*, 61(6):6914, 2000.

[12] G. Lumay and N. Vandewalle. Experimental study of the compaction dynamics for two-dimensional anisotropic granular materials. *Phys. Rev. E*, 74(2):021301, 2006.

[13] I.S. Aranson, D. Volfson, and L.S. Tsimring. Swirling motion in a system of vibrated elongated particles. *Phys. Rev. E*, 75(5):051301, 2007.

[14] A. Kudrolli, G. Lumay, D. Volfson, and L.S. Tsimring. Swarming and swirling in self-propelled polar granular rods. *Phys. Rev. Lett.*, 100(5):058001, 2008.

[15] S. Swaminathan, D. Karpeev, and I.S. Aranson. Bundle dynamics of interacting polar rods. *Phys. Rev. E*, 77(6):066206, 2008.

[16] V. Narayan, N. Menon, and S. Ramaswamy. Nonequilibrium steady states in a vibrated-rod monolayer: tetratic, nematic, and smectic correlations. *J. Stat. Mech.*, 01:P01005, 2006.

[17] P.G. DeGennes and J. Prost. *The Physics of Liquid Crystals, Second Edition*. Oxford Science Publications, 1993.

[18] C.R. Iacovella. Nematic liquid crystal, . URL `http://repository.matdl.org/repository/view/matdl:853`.

[19] S. Chandrasekhar. *Liquid Crystals, Second Edition*. Cambridge University Press, 1992.

[20] *1. A. Paramekanti, University of Toronto, pers. comm.

[21] C.R. Iacovella. Smectic a liquid crystal, . URL `http://repository.matdl.org/repository/view/matdl:864`.

[22] *2. S. Morris, A. Paramekanti, University of Toronto, pers. comm.

[23] *3. The code was originally based on magicwand2 by Yorim Tal, available at http://www.mathworks.com, but its Euclidean distance formula was not adequate to differentiate the elastics from the picture.

[24] T. Riemersma. Colour metric, September 2009. URL `http://www.compuphase.com/cmetric.htm`.

[25] R. Eppenga and D. Frenkel. Monte carlo study of the isotropic and nematic phases of infinitely thin hard platelets. *Mol. Phys.*, 52:1303, 1984.

[26] *4. Nearest neighbor searching was done using K Nearest Neighbors by Ani, found at http://www.mathworks.com.

[27] *5. Smoothing was done using MATLAB's convn function and peak detection using peakdet by Eli Billauer, found at http://www.billauer.co.il/peakdet.html.